Modeling Diffusion of Sparsely Populated Acids on a Monomer/Polymer Lattice using Monte Carlo in 3 Dimensions

Andrew Brzezinski, Matthew Duch
Dept. of Materials Science & Engineering

Spring 2006

1. Introduction & Motivation

The purpose of this project is to model the diffusion of an acid species in a chemically amplified photoresist. Acid is generated in the SU8-2000 photoresist [1] by multi-beam interference of a laser with a wavelength on the order of 351 to 532 nm, as illustrated by figure 1 below.

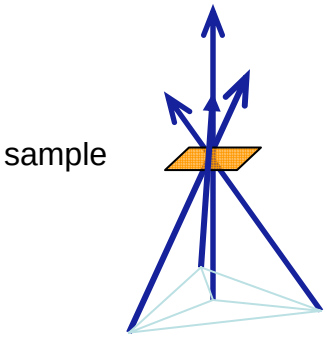

Figure 1. 4 beam interference that results in acid generation.

The resulting intensity pattern that was calculated for the face centered cubic structure, and is shown below in figure 2.

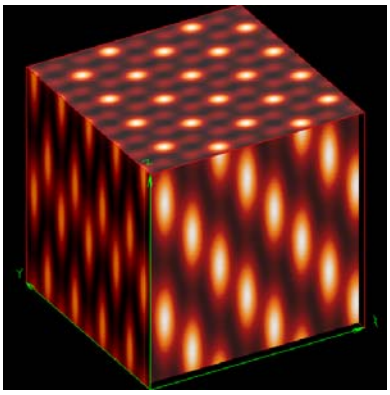

Figure 2. Interference pattern resulting from the intersection of 4 lasers.

The intensity has a profile that is very close to a Gaussian distribution. For this simulation, the intensity will be assumed Gaussian, which fits well with experimental data. Once the acid has been generated, it acts as a catalyst for cross-linking the photoresist. The acid diffuses throughout the photoresist, and experimental studies have shown the acid moves slower through the cross-linked polymer areas than in the monomer. This results in a structure as seen in figure 3.

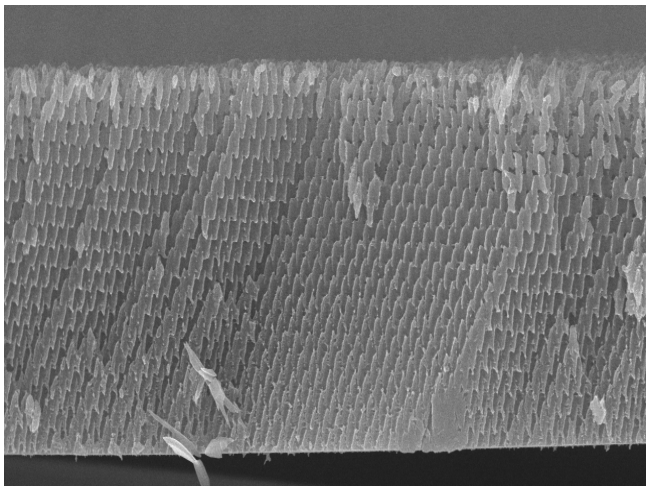

Figure 4. Image of real structure formed using this method.

Studies have been carried out on SU8 processing and developing but most of the process is poorly understood [2]. Detailed work has been performed to determine microscope diffusion of acid and the ionization of acid species in SU8 resist [2]. This work can be used to relate the simulation time to real world time. By studying the crosslinking behavior of SU8 it may be possible to use the results as a guide to setting actual experimental parameters such as exposure intensity and crosslinking time such that better structures are made.

2. Procedure

This section will cover the three main portions of the code written: the placement of acid on the lattice and the initialization of the lattice itself, the polymerization of the lattice and the movement of acids, and the tools used to determine the state of the lattice at a given timestep.

2.a. Initialization of Lattice and Acid Positions

In order to correctly simulate the cross-linking of the photoresist, it is necessary to simulate the face centered cubic (FCC) unit cell. However, this cell contains four primitive cells, which means we are simulating 4 times as many positions as are necessary. Unfortunately, the primitive cell is difficult to simulate, as it does not have a rectangular lattice. Therefore, a new lattice, only twice the size of the primitive lattice is used. This lattice is illustrated below in figure 5.

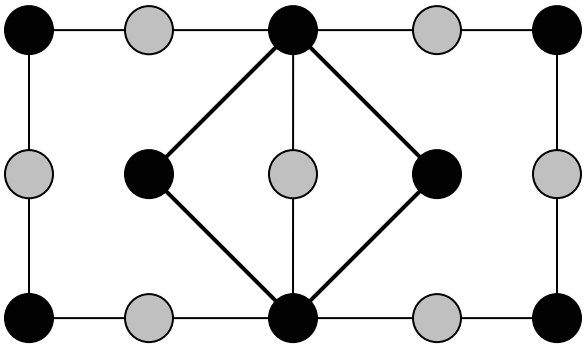

Figure 5. Crystal plan of 2 FCC unit cells. Heaver lines outline the unit cell used in the simulation. Lighter atoms denote they are at ½ of the unit cell height on the Z axis, while completely black spheres are at 0 on the Z axis.

As can be seen, the new unit cell is rectangular body centered. The height is $\sqrt{2}$ times the base length. In this simulation the dimensions of the unit cell were 400x400x566 bins, which results in a total of 90,560,000 bins. This means each bin's volume is 0.5 nm^3, around the dimensions of a monomer of the photoresist. Each bin was initialized to be a monomer.

Next, a simplifying assumption was made that the size of the acid was so much smaller than the size of the monomer that one or more acids could coexist with a monomer or polymer in each bin. The concentration of acid produced is roughly 0.1% of total bins. This means that multiple acids would rarely occupy the same space, and that the chances of the volume of the acids per bin being large enough to impact the simulation were so minute that this possibility was ignored in order to improve efficiency.

As mentioned earlier, the laser illumination intensity at each lattice point was found experimentally to have close to a Gaussian distribution. For this simulation, the contribution of 13 Gaussian distributions was used. Four of these distributions came from the plane at 0 and 1 on the Z axis (those black atoms from figure 5 above that define the corners of the unit cell used in this simulation). Next, 5 atoms from the plane ½ of the height of the unit cell were used (the gray atom in the center of the unit cell and the four nearest neighbors on that plane). All other contributions to the intensity distribution did not have any serious impact on the final intensity distribution and were ignored. The intensity was scaled to a factor determined at runtime. Acids were placed randomly as determined by the probability distribution which is proportional to the intensity.

2.b. Polymerization of Lattice and Movement of Acids

In this simulation, polymerized areas of the photoresist are assumed to not move, as they are fixed by cross-linking. Also, if a monomer moves, it can only exchange places with another monomer, so its movement can be ignored. This results in a model where the only movement is acid movement. In this model, acid movement is assumed to have no energy cost associated with it when moving onto a monomer space. However, there is an energy penalty for moving into a cross-linked area, as the polymerization cuts down on the possible movements.

Therefore, when moving onto a monomer bin, the probability of accepting the move is 1. However, whenever moving into a polymer bin, the probability of movement is a fixed parameter. The value of this parameter must be fitted to experimental data as there is not enough literature on this topic to determine it analytically. Also, the probability of an acid polymerizing a given monomer bin is another parameter that must be fitted, as the reaction of this catalyst and monomer is poorly understood.

Applying the Monte Carlo method using these movement parameters and periodic boundary conditions results in the evolution of our model. A list of acids is maintained to improve efficiency of the code, so all cells do not need to be checked, but acids are directly selected. The list of acids is traversed. The probability of polymerizing the current bin (if the bin is a polymer) is compared to a random number and the polymerization process is rejected or accepted. A random direction is selected. If the movement is onto a monomer, the chance of moving is one, and the acid is moved. Otherwise, the probability of moving into a polymer bin is compared to a random number and the movement is either rejected or accepted.

2.c. Determination of Lattice State at a Given Timestep

The analysis of the results produced by this simulation is meaningful only in terms several values regarding the clusters formed. The number of clusters, the size distribution of the clusters, and the average number of bonds in each cluster give insight as to the state of the unit cell. The algorithm employed to determine these values is summarized below.

The algorithm begins at a polymer, and labels it a number, while modifying the values for this label to account for the number of bonds. All neighbors are examined in this way, and labels added, and values of the label updated. If a polymer encountered already contains a label, the label of the neighbor of this polymer is updated to point to the current polymer’s label as a root.

Once all polymers have been labeled, it is easy to collapse all labels to their roots, and the size and average number of bonds in the cluster (root) can be determined.

3. Results & Discussion

This section will cover the two main portions of the application of the code: determination of polymer movement penalty and polymerization rate values, and application to determine the effects of illumination intensity and cross-linking time.

3.a. Determination of Polymer Movement Penalty and Polymerization Rate

In order to determine the effects of the polymerization rate on the evolution of a simulation run, the movement probability into a polymerized region was kept at 0.3 while the polymerization probability was set to 0.25, 0.5, 0.75, and 1.0. The number of polymerized sites with 0,1,2,3,4,5, and 6 bonds (neighboring bins that are also polymerized) was recorded. The results are shown below in figure 6 for the simulation with a polymerization probability of 0.25.

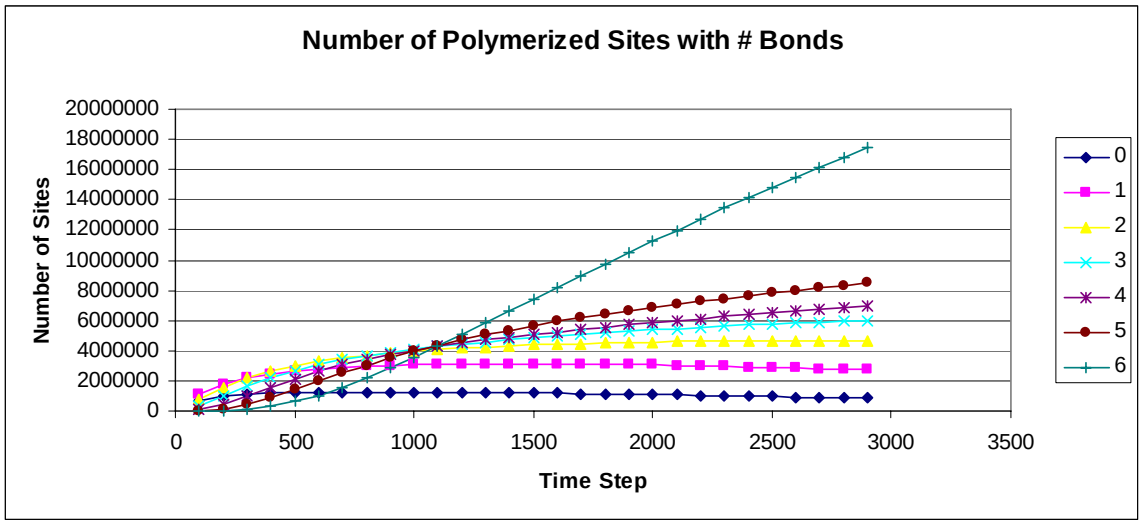

Figure 6. The number of polymerized sites as a function of timestep for each bond number with a polymerization probability of 0.25.

Initially, the number of sites with 1 neighbor that is polymerized dominates, but eventually there is a crossover and the largest number of sites has polymerized neighbors in all 6 directions. As the polymerization rate increases, the number of sites with six bonds becomes larger at a faster rate. This is expected as a larger number of sites should be polymerized, and there is also a greater likelihood for more polymerized neighbors.

The total number of clusters as a function of time was also analyzed. The results for the sample with a polymerization rate of 0.25 is shown below in figure 7.

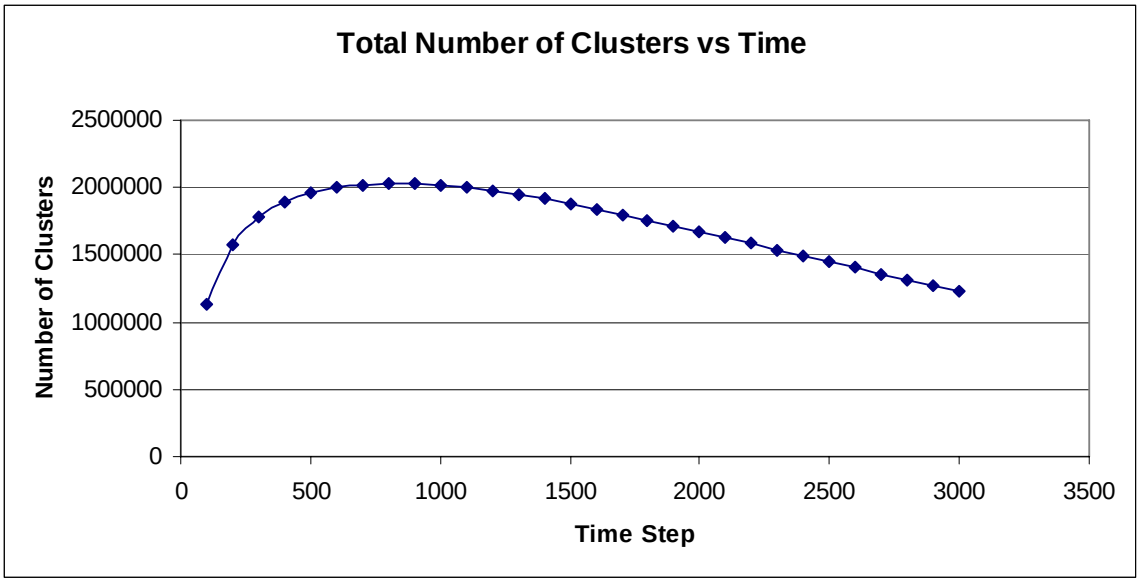

Figure 7. Number of clusters as a function of time with a polymerization rate of 0.25.

The number of clusters increases as the number of timesteps increases, initially. This function exhibits a peak and the drops off. As the polymerization probability increases this peak occurs earlier, is sharper, and drops off more quickly. At a polymerization probability of 1.0, the value after 100 timesteps is the peak (already an order of magnitude lower than the peak seen in the sample with a 0.25 polymerization probability) and drops to under 100,000 clusters by the next value.

Finally, the largest cluster size as a function of timestep was recorded. For the simulation with a polymerization probability of 0.25 the results are shown in figure 8.

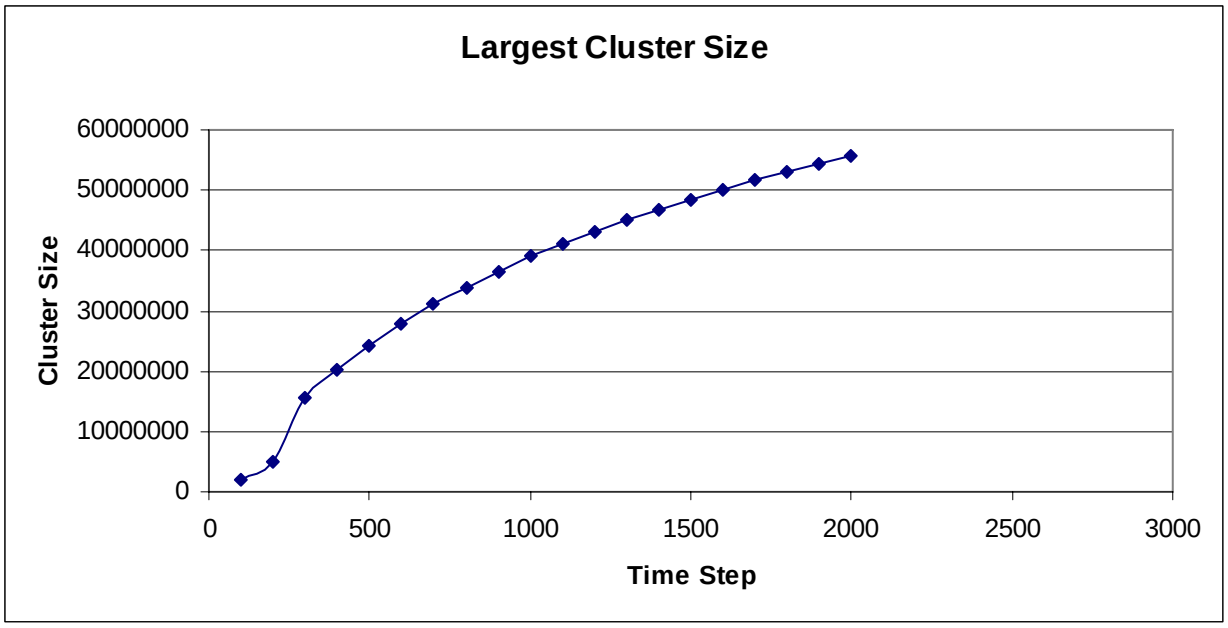

Figure 8. Largest cluster size as a function of time step for the simulation with a polymerization probability of 0.25.

The most interesting feature of this plot is the transition jump at around the same time as the peak in the number of clusters. This indicates a critical point at which clusters rapidly begin to join together. As with the peak in the number of clusters, this transition point occurs earlier as the polymerization probability increases.

After examining the evolution of the unit cell, better results are achieved using polymerization probabilities in the middle rage (~0.5). With lower probabilities the evolution is very slow and very sparsely populated. With larger probabilities, acids leave chains of polymerized bins, which does not fit well with polymerization patterns observed.

The effects of the movement rate into polymerized regions was studied by keeping the polymerization probability at 0.5 and setting the movement probability into polymerized regions to 0.0, 0.3, 0.5, 0.7, and 1.0. Analysis of structure evolution was carried out as before (studying cluster size, number of bonds per polymerized site, and number of clusters) and compared to experimental results.

When movement into polymerized regions was not allowed (movement probability of 0.0) the number of polymerized sites with a certain number of bonds produced interesting results.

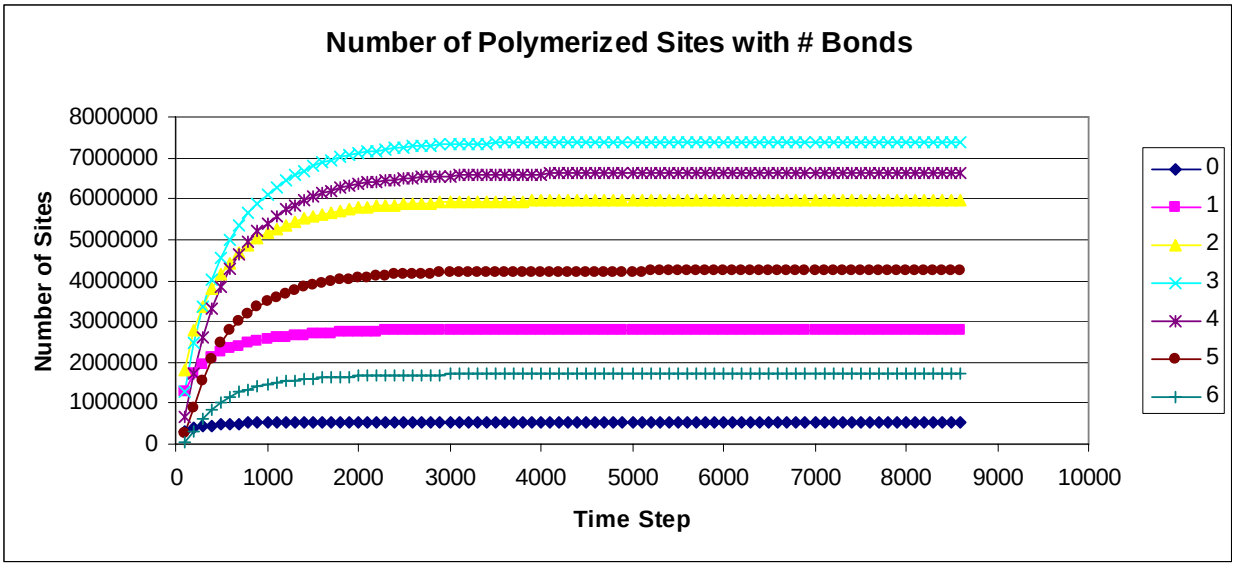

Figure 9. The number of polymerized sites as a function of timestep for each bond number with a movement probability of 0.0.

In this case, the most common bond number was 3, as opposed to the 6 that eventually becomes the most common number. This is most likely due to pockets of monomer becoming trapped in polymerized regions so movement into these regions by acids becomes impossible. This does not fit experimental data. Data for other movement probabilities fit experimental data fairly well. As the movement rate increased, the number of clusters decreased for a given timestep. This results in a more interconnected structure at earlier times. This is a reasonable result so it is not possible to rule out any movement probabilities into polymerized bins based on the analysis carried out. This is most likely very dependant on temperature, so different movement probabilities simply reflect higher temperatures. However, one of the few known facts of this process is that the acid does travel slower in polymerized regions, so the value must be less than one. Based on these considerations, a reasonable value of 0.5 was chosen for the rest of this experiment.

3.b. Effects of Illumination Intensity and Cross-Linking Time

Simulations were run with intensities I_0, 2 I_0, 4 I_0, 8 I_0, and 16 I_0. The highest intensities were those were the difference between the lightest area and darkest area was smallest. The polymerization probability was 0.5 and the movement probability into polymerized areas was 0.3, with the justification being presented in the previous section. Several clear trends were visible in the largest cluster size as a function of timestep and number of sites grouped by number of bonds. The largest cluster size as a function of timestep comparison is shown below in figure 10.

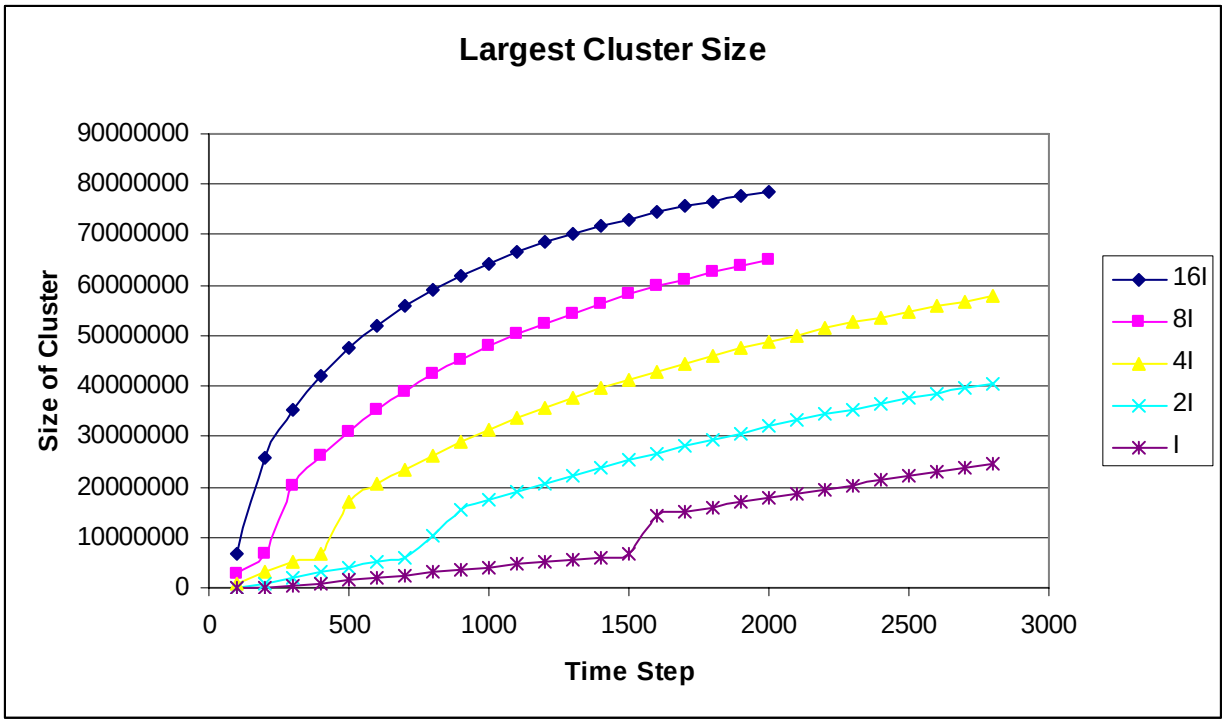

Figure 10. Largest cluster size as a function of timestep.

As can be seen from figure 10, the transition when individual lattice points form an interconnected structure occurs at a later time and over a longer time for lower intensities. Also, with higher intensities, the largest cluster size grew far more rapidly and achieved much higher cluster sizes, approaching a final curve similar to a logarithmic.

Next, the number of sites grouped by number of bonds as a function of timestep was examined. The results are shown in figure 11.

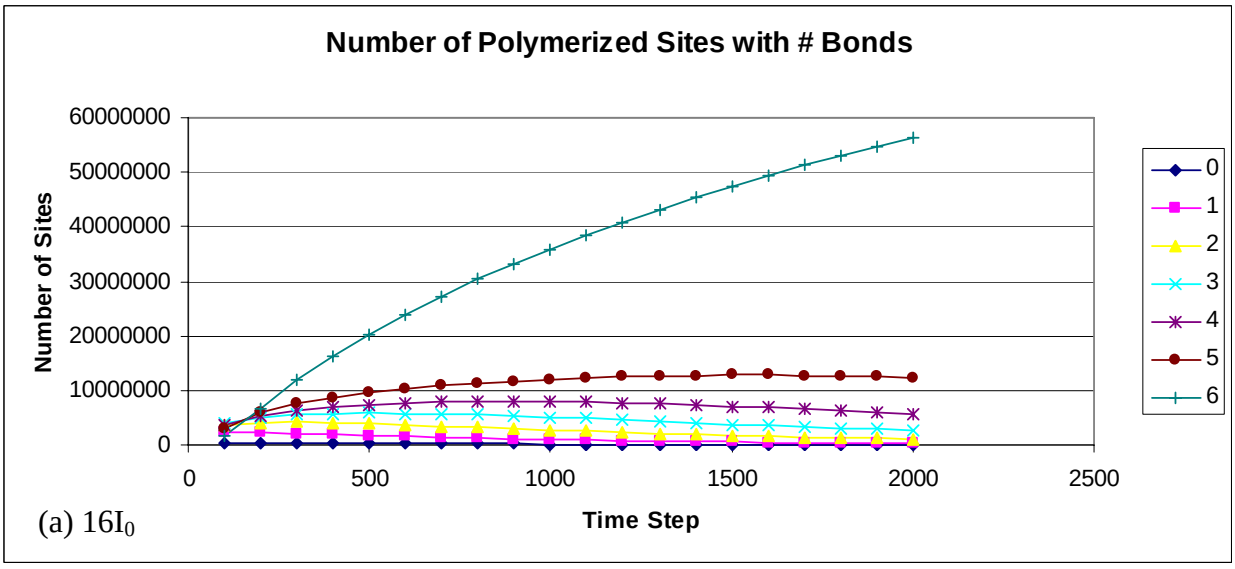

(a) $16I_0$

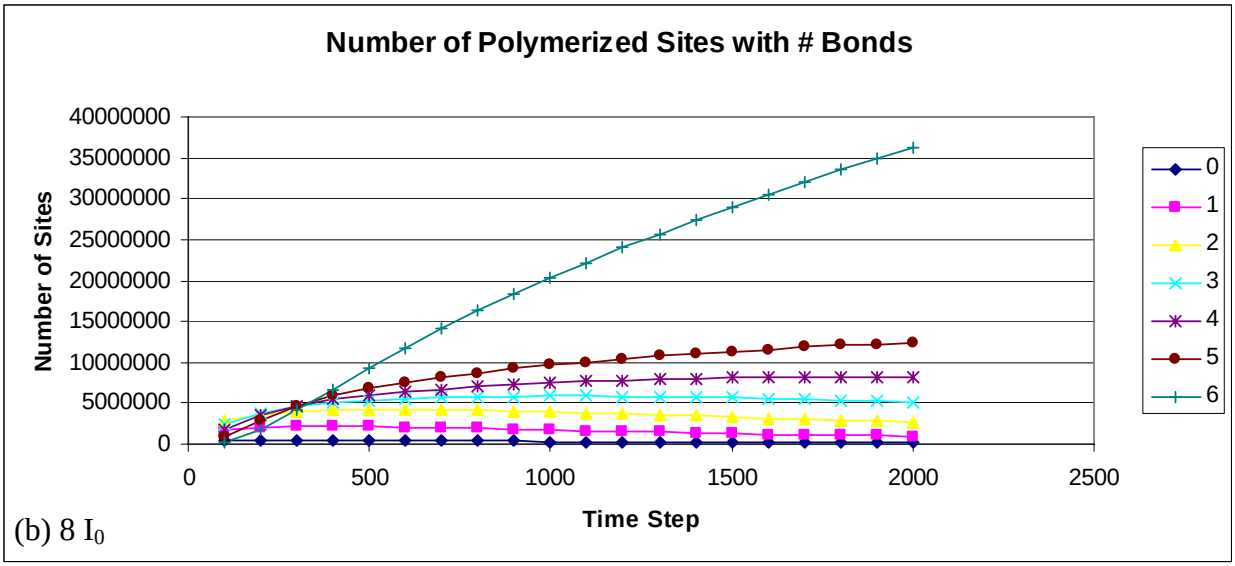

(b) 8 I_0

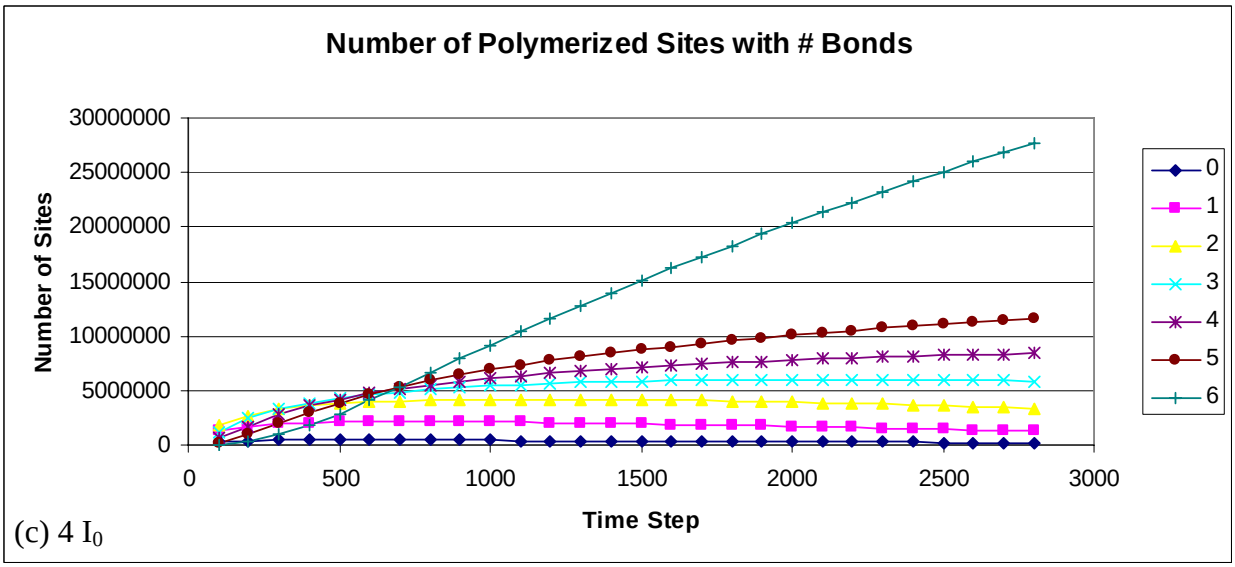

(c) 4 I_0

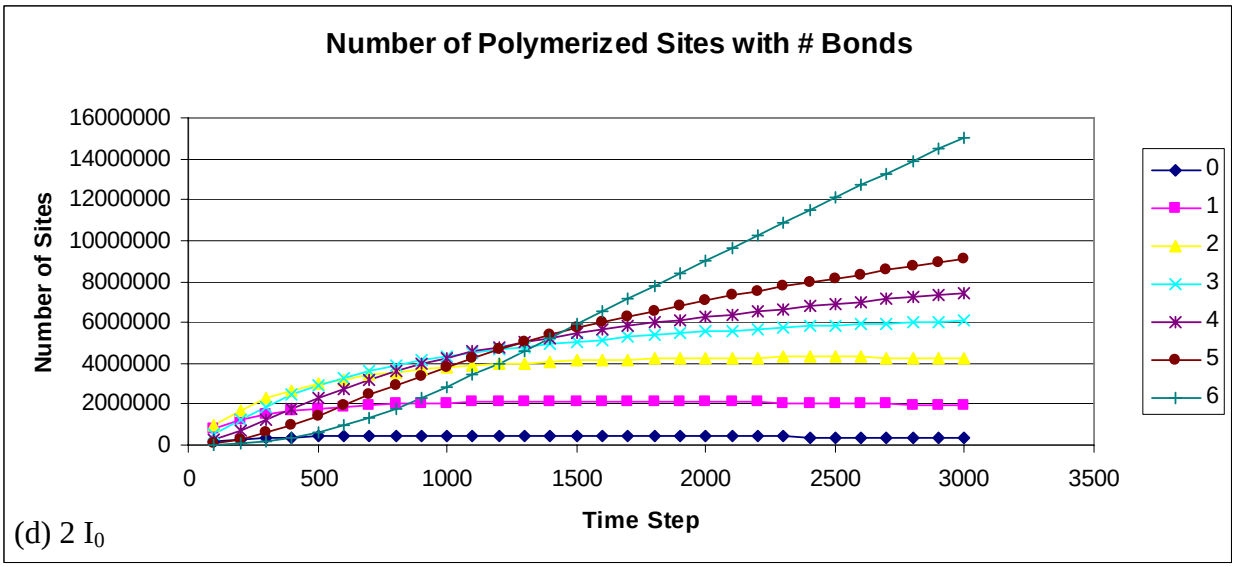

(d) 2 I_0

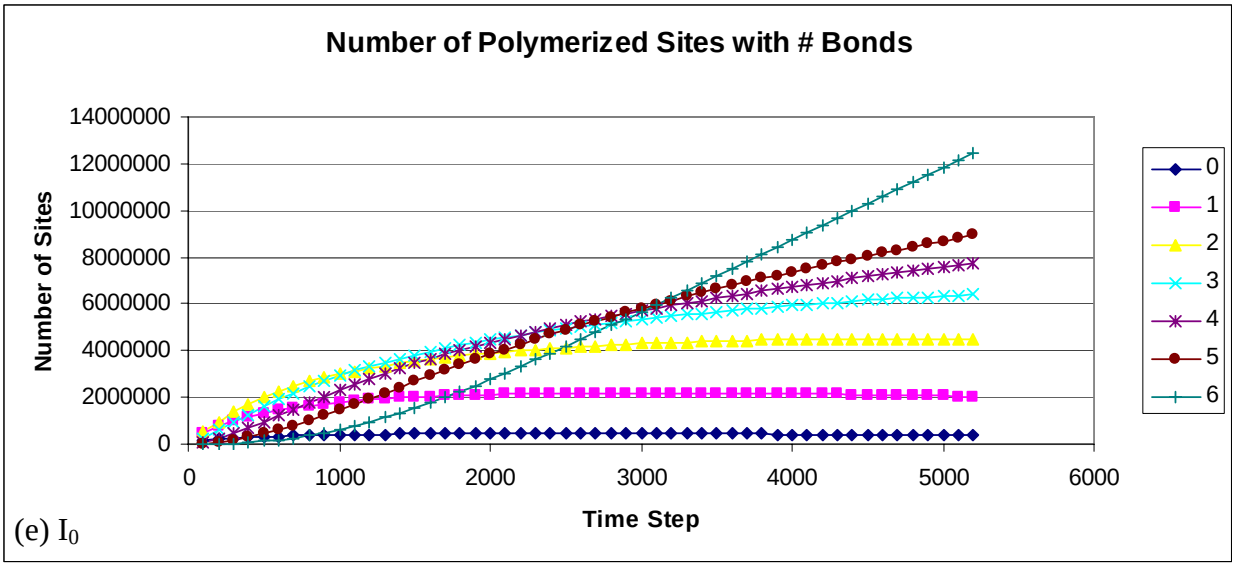

Figure 11. Number of polymerized sites grouped by number of bonds. Results for intensity contrasts of (a) 16 I_0, (b) 8 I_0, (c) 4 I_0, (d) 2 I_0, and (e) I_0.

These plots show how, at higher intensities, the group of sites with 6 bonds dominates the total number of polymerized sites. At lower intensities, although the group of sites with 6 bonds eventually becomes the largest fraction, it occurs at later times and is not as dominant of a fraction. At low intensities, the number of sites with 0 or 1 bonds stays fairly constant, dropping only slightly, while at higher intensities these values approach 0 at a higher rate.

Another analysis is the number of clusters of a given size as a function of timestep. Clusters were binned by size on a logarithmic scale. The results are shown in figure 12.

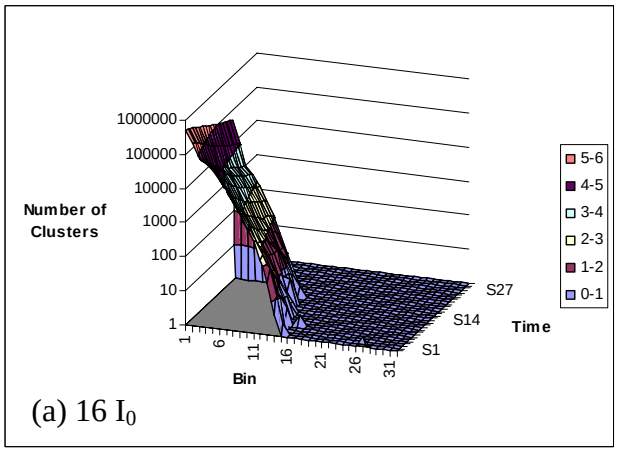

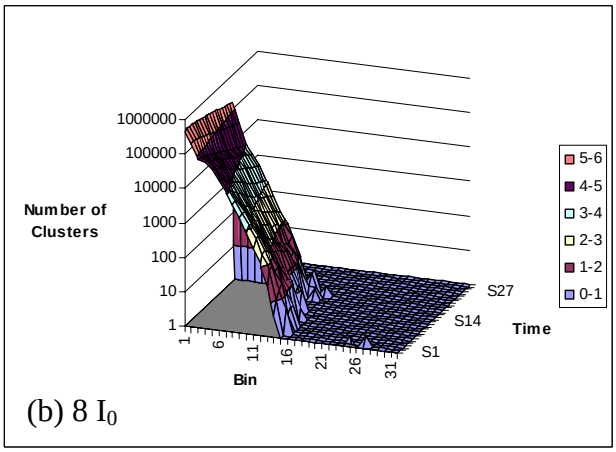

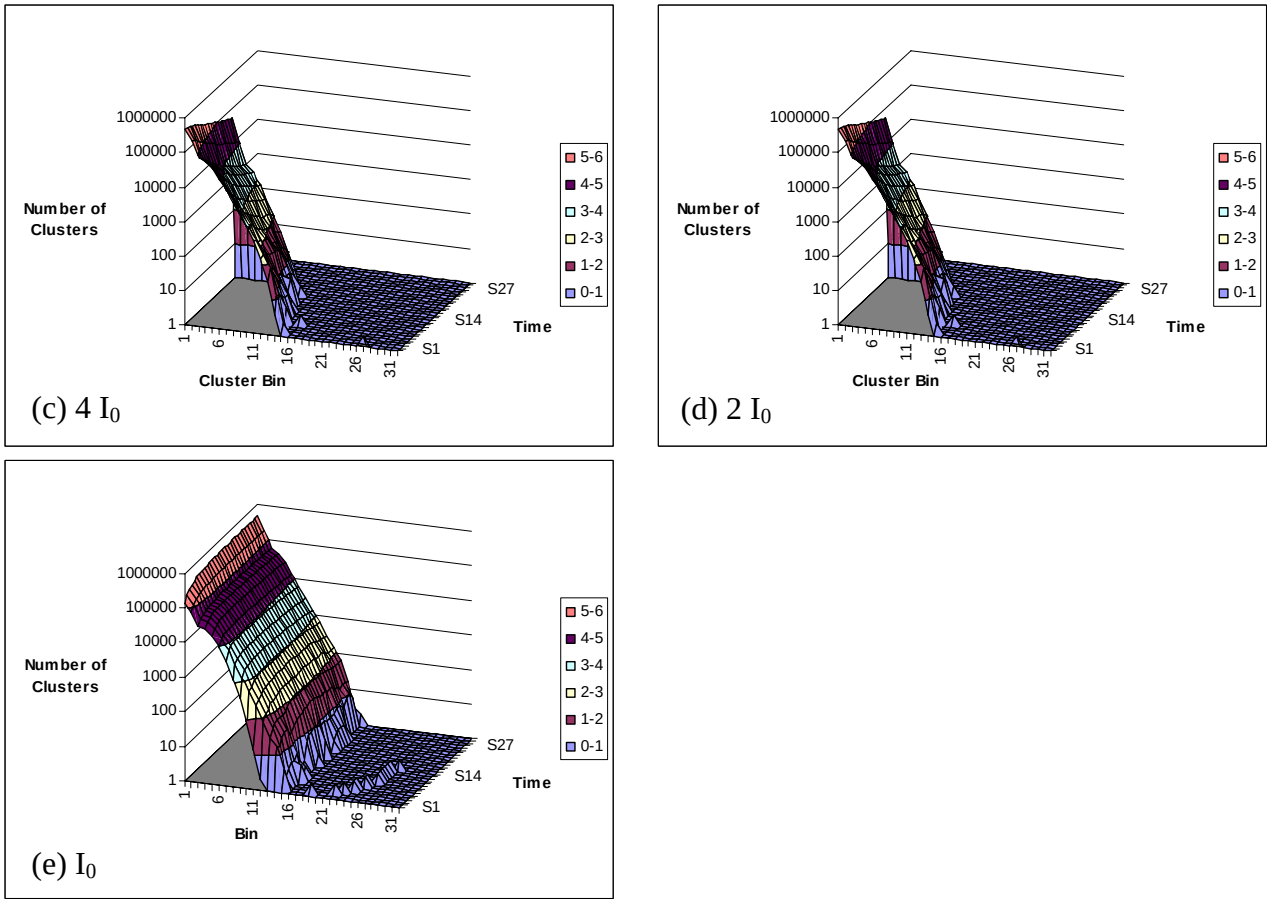

Figure 12. Number of clusters (on a logarithmic scale) binned by time and logarithmic cluster size for intensities (a) 16 I_0, (b) 8 I_0, (c) 4 I_0, (d) 2 I_0, and (e) I_0.

The general trend in these plots is for the number of clusters of smaller sizes to slowly decrease, while those in the middle range (bins 5-15) tend to decrease at a much faster rate, most likely due to the connection with other clusters of similar size. Large clusters are not visible as there are only a few of them, which eventually join into one big cluster, not visible on these plots.

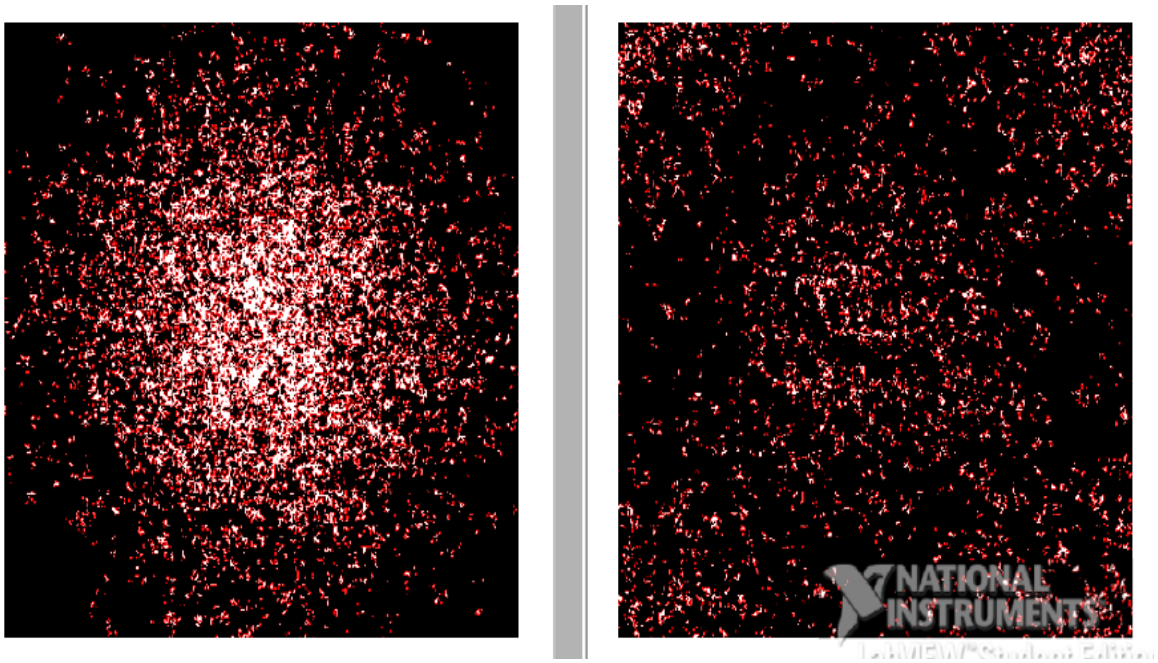

Figure 13. Lattice cross-section showing octahedral (left) and tetrahedral (right) holes after 200 time steps.

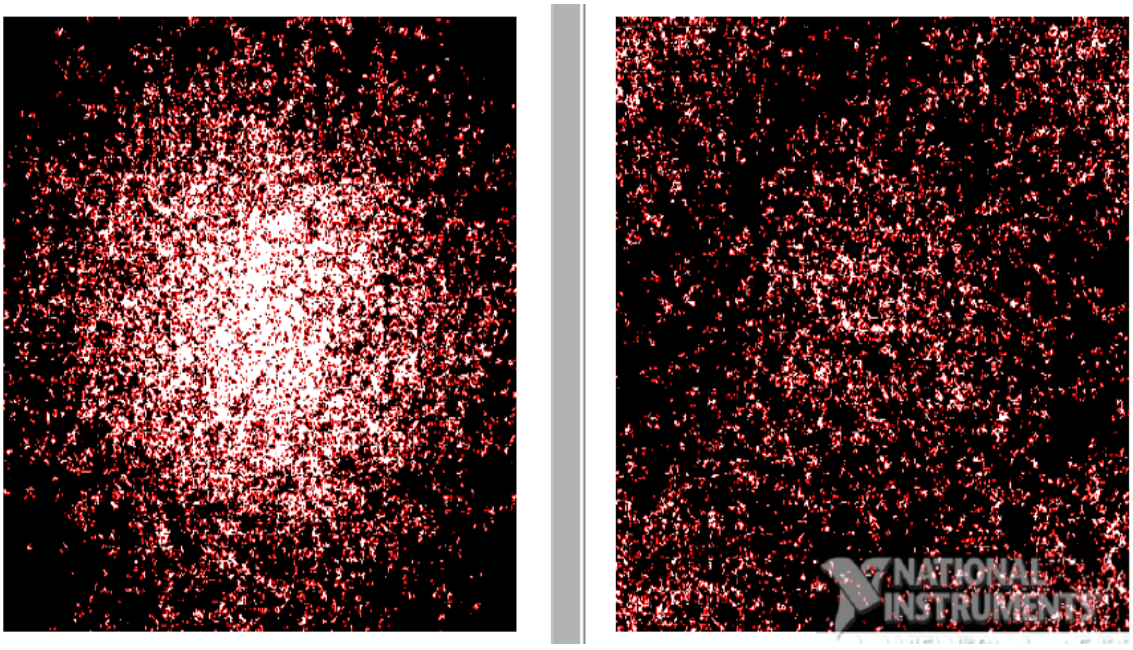

Figure 14. Lattice cross-section showing octahedral (left) and tetrahedral (right) holes after 600 time steps.

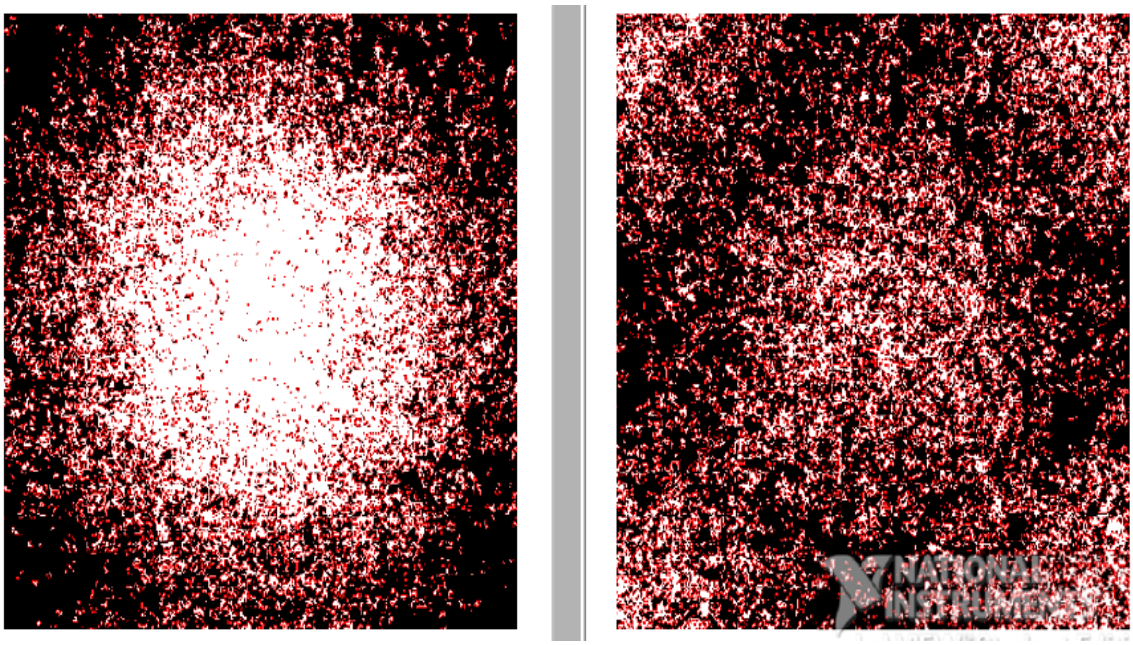

Figure 15. Lattice cross-section showing octahedral (left) and tetrahedral (right) holes after 1000 time steps.

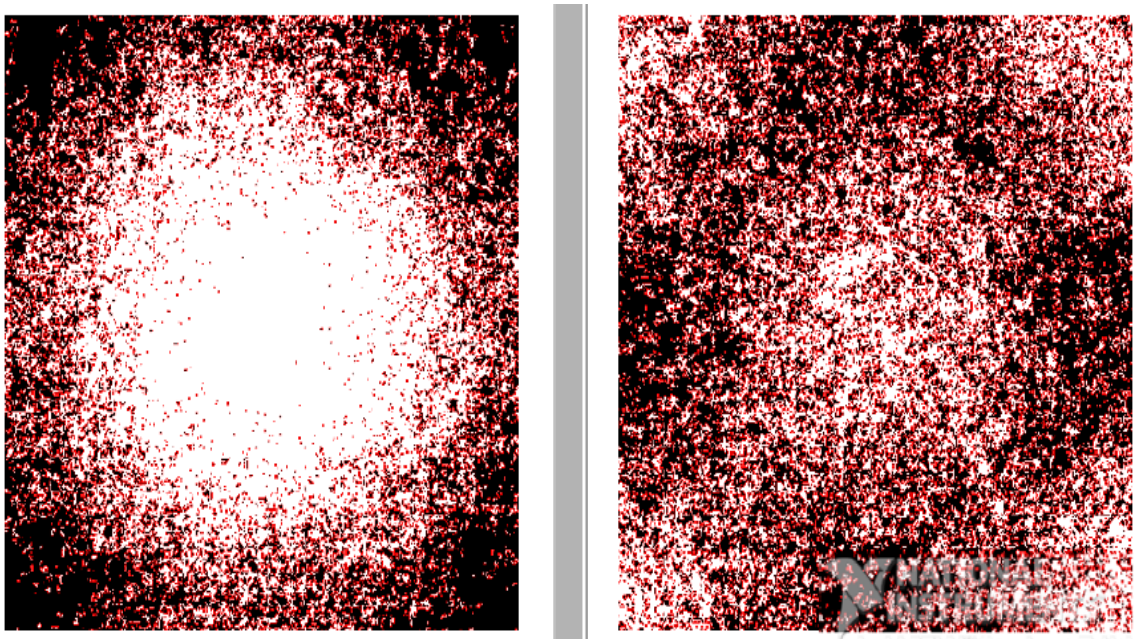

Figure 16. Lattice cross-section showing octahedral (left) and tetrahedral (right) holes after 1800 time steps.

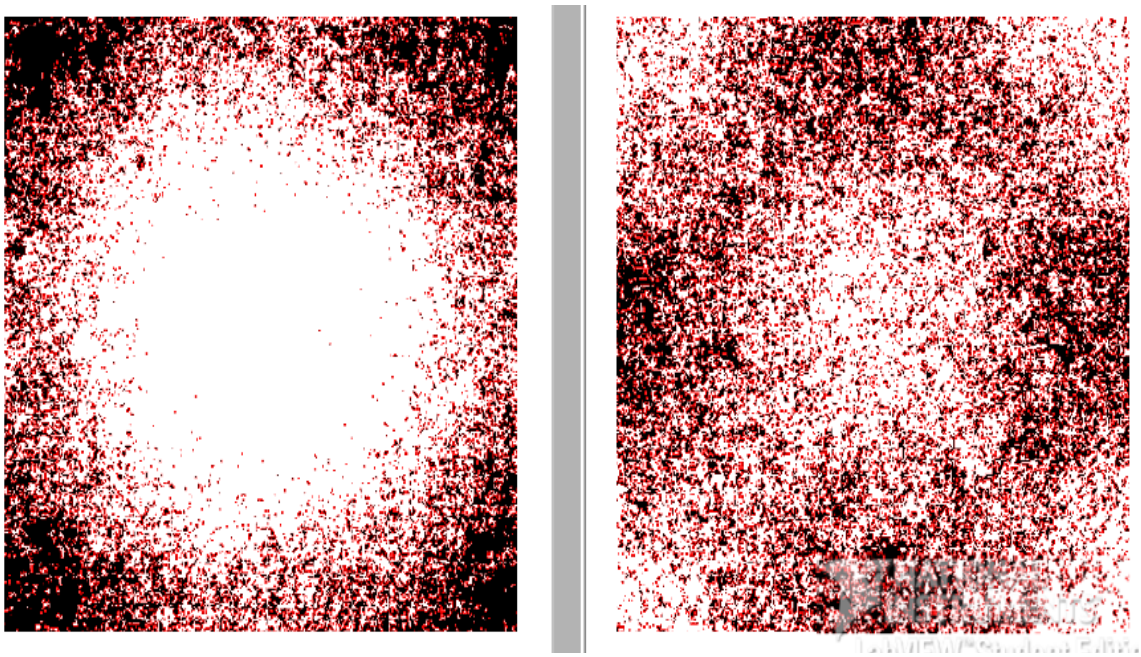

Figure 17. Lattice cross-section showing octahedral (left) and tetrahedral (right) holes after 3000 time steps.

4. Conclusions & Final Remarks

We have made a model that captures the basic physics of the SU8 crosslinking behavior. This model was used with an intensity pattern related to three dimensional interference lithography and the effect of changing exposure intensity and crosslinking time was examined. It has been determined that this model can potentially guide researchers in choosing experimental parameters for fabrication of structures in SU8 photoresist.

5. References

[1] J. M. Shaw, et. al "Negative photoresists for optical lithography", IBM Journal of Research and Development; 41 (1997) 81

[2] D. Mason, et. al. "Single Molecule Acid-Base Kinetics and Thermodynamics" PHYSICAL REIEW LETTERS, 93 (2004) 73004